Chapter 9

Synopsis

Power devices are required for systems that operate over a broad spectrum of power levels and frequencies as discussed in the textbook[1]. The wide range of operating frequency for these applications was illustrated in Fig. 1.1. Another classification for the applications that is useful is based up on the operating voltage level as shown in Fig. 9.1. At lower voltages (< 100 voltages), a large number of power rectifiers are needed for computer power supplies and in automotive electronics. Rectifiers with larger voltage ratings are required for many other applications, such as motor drives, shown in the figure.

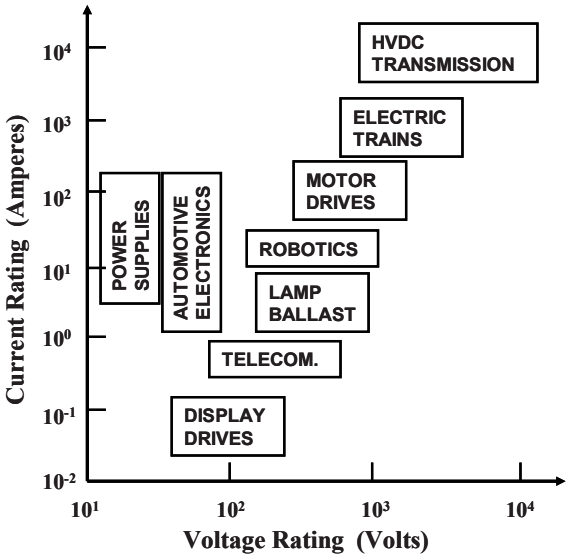

Fig. 9.1 System ratings for Power Devices.

B.J. Baliga, *Advanced Power Rectifier Concepts*, DOI: 10.1007/978-0-387-75589-2_9,

A variety of advanced power rectifier structures were discussed in previous chapters of this book for serving the applications shown in Fig. 9.1. The choice of the optimum device suitable for each application depends upon the device voltage rating and the circuit switching frequency. In the case of applications with low operating voltages (< 100 volts), silicon Schottky rectifiers have been commonly used due to their low on-state voltage drop. A typical example is the DC-to-DC buck converter circuit shown in Fig. 1.12 used as Voltage Regulator Modules (VRMs). However, the reduction of power losses in this application is limited by the large leakage current for silicon Schottky rectifiers. The performance of these devices can be improved up on by using the Junction Barrier controlled Schottky (JBS) rectifier concept discussed in chapter 3.

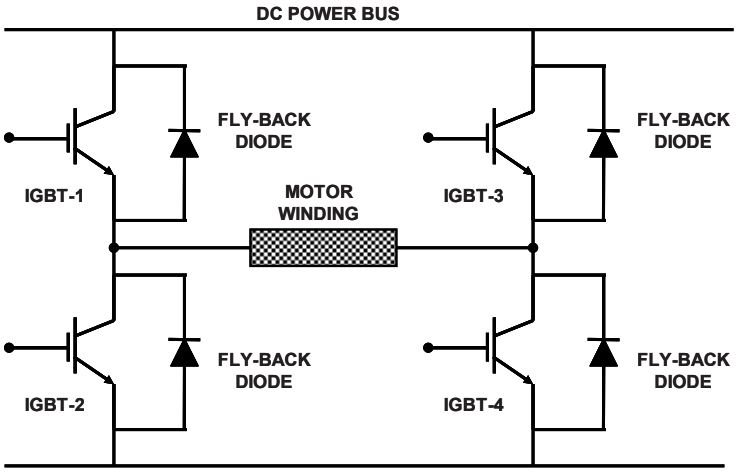

Fig. 9.2 Typical H-Bridge Topology for Motor Control.

Power rectifiers are also commonly used in motor control circuits. The most prevalent applications for commercial and industrial systems utilize silicon IGBTs as the power switch and silicon P-i-N rectifiers as the fly-back diodes with an H-bridge configuration as shown in Fig. 9.2. The operating voltages for these applications typically range from 300 volts to 6000 volts. At these voltage levels, the silicon MPS rectifier, discussed in chapter 7 of this book, provides an alternative to the P-i-N rectifier for reducing the power loss not only in the rectifiers but also in the IGBTs. In addition, an even greater improvement in performance can be obtained by utilizing the silicon carbide JBS rectifier that was discussed in chapter 3.

In this concluding chapter, an example of the performance enhancement that can be obtained by replacing the silicon Schottky rectifier with the silicon JBS rectifier in VRMs is provided. This is followed by an example of a typical motor control application to quantify the benefits of replacing the silicon P-i-N rectifier with the silicon MPS rectifier and the silicon carbide JBS rectifier.

9.1 DC-to-DC Buck Converter Application

The basic DC-to-DC buck converter circuit is shown in Fig. 1.12. In this circuit, current flow through the output inductor is provided for a part of the cycle through the power MOSFET. During the rest of the cycle, the current in the inductor circulates through the rectifier. The current and voltage waveforms for the rectifier in this circuit are illustrated in Fig. 9.3.

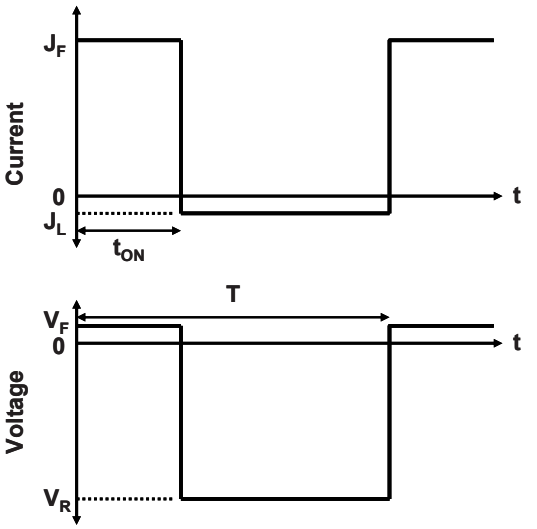

Fig. 9.3 Typical Switching Waveforms for the Rectifier.

As shown in Fig. 9.3, typical Schottky rectifiers exhibit a voltage drop (V_F) during current conduction in the forward direction. This results in power dissipation per unit area in the on-state given by:

$$P_L(on) = \delta . J_F . V_F \qquad \textbf{[9.1]}$$

where J_F is the on-state current density. In this expression, δ is referred to as the duty cycle given by:

$$\delta = t_{ON} / T \qquad \textbf{[9.2]}$$

where t_{ON} is the on-state duration and T is the time period (the reciprocal of the operating frequency). The on-state power dissipation decreases with increasing temperature because the on-state voltage drop decreases with increasing temperature for Schottky rectifiers.

The power dissipation per unit area in the off-state is given by:

$$P_L(off) = (1-\delta) . J_L . V_R \qquad \textbf{[9.3]}$$

where J_L is the leakage current density exhibited by the device in its off-state due to supporting a reverse bias (V_R). The power dissipation in the off-state increases with temperature due to a rapid increase in the leakage current for Schottky rectifiers.

The total power dissipation incurred in the diode is obtained by combining these terms:

$$P_L(total) = P_L(on) + P_L(off) \qquad \textbf{[9.4]}$$

As the temperature of the diode is increased from room temperature, the on-state power dissipation decreases resulting in a reduction of the total power dissipation because the leakage current is small. However, the leakage current increases rapidly at high temperatures resulting in an increase in the power dissipation with temperature. Consequently, the power dissipation in the Schottky rectifier goes through a minimum with increasing temperature as illustrated in Fig. 9.4 for the case of a device with breakdown voltage of 50 volts. A duty cycle of 10 percent was used in this example as representative of the buck converter operating with a ratio of the DC input voltage to output DC voltage of 10. The Schottky barrier height was adjusted to obtain a minimum power dissipation at 400 ^{o}K. A reverse bias voltage of 50 volts and an on-state current density of 100 A/cm^2 were assumed for this example. The impact of Schottky barrier lowering and pre-breakdown avalanche multiplication were taken into account during the analysis.

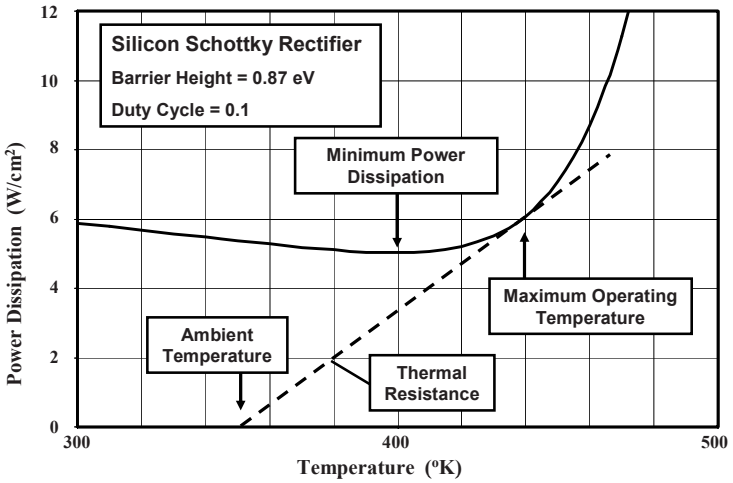

Fig. 9.4 Typical Power Dissipation for a Silicon Schottky Rectifier.

The maximum stable operating temperature for the Schottky rectifier is limited by the thermal impedance of the package and heat sink. If a tangent is drawn from the ambient temperature to the power dissipation curve as shown in Fig. 9.4, the maximum stable operating temperature of 440 ^{o}K is obtained as shown in the figure. Although stable operation is theoretically predicted below this

temperature point, it is prudent to keep the maximum operating temperature below the point of minimum power dissipation indicated in the figure. The lowest power dissipation is 5 W/cm^2 for the Schottky rectifier in this example.

The replacement of the silicon Schottky rectifier with the JBS rectifier enables a reduction of the power dissipation because the leakage current is suppressed in the JBS rectifier structure. Judicious choice of the structural dimensions of the JBS rectifier structure is required to achieve an improved performance. Consider the case of a JBS rectifier with the same breakdown voltage of 50 volts as the Schottky rectifier and operating in the same DC-to-DC converter with the same duty cycle of 10 percent (a ratio of the DC input voltage to output DC voltage of 10). Assuming the same reverse bias voltage of 50 volts and an on-state current density of 100 A/cm^2 and after including the impact of less Schottky barrier lowering due to the shielding by the junction, the calculated power dissipation is shown in Fig. 9.5 as a function of temperature. Three device structures were considered in this analysis with different cell pitch while keeping the width of the diffusion window (s) at 0.25 microns and the depth of P^+ region at 0.5 microns. The Schottky barrier height in the JBS rectifier structure was reduced to 0.77 eV to achieve a minimum power dissipation at the same temperature (400 ^{o}K) as observed for the Schottky rectifier. It can be concluded that the lowest power dissipation is 4.5 W/cm^2 for the JBS rectifier with a cell pitch of 1.25 to 1.5 microns in this example. This demonstrates that a reduction in power losses by about 10 percent is feasible using this technology. Note that when the cell pitch is reduced to 1.00 microns in the JBS rectifier structure, the minimum power dissipation exceeds that observed for the Schottky rectifier.

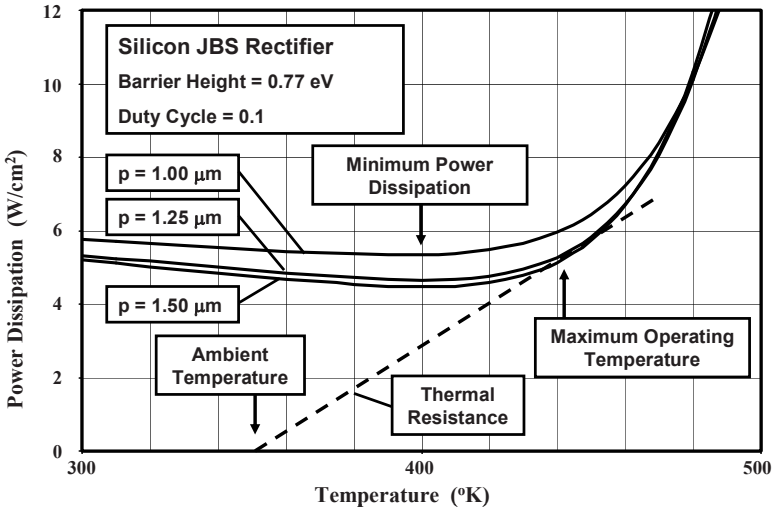

Fig. 9.5 Power Dissipation for Silicon JBS Rectifiers.

9.2 Typical Motor Control Application

The control of motors using PWM circuits is typically performed using the H-bridge configuration shown in Fig. 9.2. In this figure, the circuit has been implemented using four IGBT devices as the switches and four P-i-N rectifiers as the fly-back diodes. This is the commonly used topology for medium and high power motor drives where the DC bus voltage exceeds 200 volts. The direction of the current flow in the motor winding can be controlled with the H-bridge configuration. If IGBT-1 and IGBT-4 are turned-on while maintaining IGBT-2 and IGBT-3 in their blocking mode, the current in the motor will flow from the left-side to the right-side in the figure. The direction of the current flow can be reversed if IGBT-3 and IGBT-2 are turned-on while maintaining IGBT-1 and IGBT-4 in their blocking mode. Alternately, the magnitude of the current flow can be increased or decreased by turning on the IGBT devices in pairs. This method allows synthesis of a sinusoidal waveform across the motor windings with a variable frequency that is dictated by the PWM circuit[2].

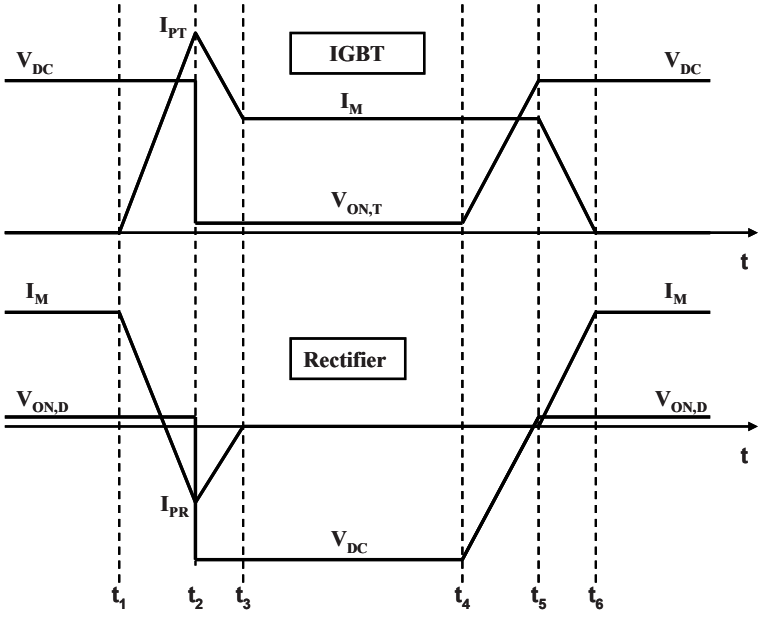

Fig. 9.6 Typical Waveforms during PMW Operation.

The typical waveforms for the current and voltage across the power transistor and the fly-back diode are illustrated in Fig. 9.6 during just one cycle of the PWM operation. These waveforms have been linearized for simplification of the analysis[3]. The cycle begins at time t_1 when the transistor is turned-on by its gate drive voltage. Prior to this time, the transistor is supporting the DC supply voltage and the fly-back diode is assumed to be carrying the motor current. As the

transistor turns-on, the motor current is transferred from the diode to the transistor during the time interval from t_1 to t_2. In the case of high DC bus voltages, where P-i-N rectifiers are utilized, the fly-back diode will not be able to support voltage until the stored charge in its drift region is removed as discussed in chapter 6. In order to achieve this, the P-i-N rectifier must undergo its reverse recovery process. During reverse recovery, substantial reverse current flows through the rectifier with a peak value I_{PR} reached at time t_2. The large reverse recovery current produces significant power dissipation in the diode. Moreover, the current in the IGBT at time t_2 is the sum of the motor winding current I_M and the peak reverse recovery current I_{PR}. This produces substantial power dissipation in the transistor during the turn-on transient. The power dissipation in both the transistor and the diode are therefore governed by the reverse recovery characteristics of the power rectifier.

The power transistor is turned-off at time t_4 allowing the motor current to transfer from the transistor to the diode. In the case of an inductive load, such as motor windings, the voltage across the transistor increases before the current is reduced, as illustrated in Fig. 9.6 during the time interval from t_4 to t_5. Subsequently, the current in the transistor reduces to zero during the time interval from t_5 to t_6. The turn-off durations are governed by the physics of the transistor structure as discussed in previous chapters. Consequently, the power dissipation in both the transistor and the diode during the turn-off event are determined by the transistor switching characteristics.

In addition to the power losses associated with the two basic switching events within each cycle, power loss is incurred within the diode and the transistor during their respective on-state operation due to a finite on-state voltage drop. It is common practice to trade off a larger on-state voltage drop to obtain a smaller switching loss in the bipolar power devices. Consequently, the on-state power loss cannot be neglected especially if the operating frequency is low. The leakage current for the devices is usually sufficiently small so that the power loss in the blocking mode can be neglected.

The total power loss incurred in the power transistor can be obtained by summing four components:

$$P_{L,T}(total) = P_{L,T}(on) + P_{L,T}(off) + P_{L,T}(turnon) + P_{L,T}(turnoff) \qquad \textbf{[9.5]}$$

The power loss incurred in the transistor during the on-state duration from time t_3 to t_4 is given by:

$$P_{L,T}(on) = \frac{(t_4 - t_3)}{T}.I_M.V_{ON,T} \qquad \textbf{[9.6]}$$

The power loss incurred in the transistor during the off-state duration beyond time t_6 until the next turn-on event is given by:

$$P_{L,T}(off) = \frac{(T - t_6)}{T}.I_{L,T}.V_{DC} \qquad \textbf{[9.7]}$$

The leakage current ($I_{L,T}$) for the transistors is usually very small allowing this term to be neglected during the power dissipation analysis.

The power loss incurred in the transistor during the turn-on event from time t_1 to t_3 can be obtained by analysis of the segments between the time intervals t_1 to t_2 and t_2 to t_3. The power loss incurred during the first segment is given by:

$$P_{L,T-1}(turnon) = \frac{1}{2}\frac{(t_2 - t_1)}{T}.I_{PT}.V_{DC} \quad \textbf{[9.8]}$$

where the peak transistor current is dependent on the peak reverse recovery current of the P-i-N rectifier:

$$I_{PT} = I_M + I_{PR} \quad \textbf{[9.9]}$$

In the power loss analysis, it will be assumed that the time duration ($t_2 - t_1$) is determined by the reverse recovery behavior of the P-i-N rectifier and is independent of the operating frequency. The power loss incurred during the second segment is given by:

$$P_{L,T-2}(turnon) = \frac{1}{2}\frac{(t_3 - t_2)}{T}.\left(\frac{I_{PT} + I_M}{2}\right).V_{DC} \quad \textbf{[9.10]}$$

In the power loss analysis, it will be assumed the time duration ($t_3 - t_2$) is also determined by the reverse recovery behavior of the P-i-N rectifier and is independent of the operating frequency.

The power loss incurred in the transistor during the turn-off event from time t_4 to t_6 can be obtained by analysis of the segments between the time intervals t_4 to t_5 and t_5 to t_6. The power loss incurred during the first segment is given by:

$$P_{L,T-1}(turnoff) = \frac{1}{2}\frac{(t_5 - t_4)}{T}.I_M.V_{DC} \quad \textbf{[9.11]}$$

The time interval ($t_5 - t_4$) is determined by the time taken for the transistor voltage to rise to the DC power supply voltage. The power loss incurred during the second segment is given by:

$$P_{L,T-2}(turnoff) = \frac{1}{2}\frac{(t_6 - t_5)}{T}.I_M.V_{DC} \quad \textbf{[9.12]}$$

The time interval ($t_6 - t_5$) is determined by the time taken for the transistor current to decay to zero.

In a similar manner, the total power loss incurred in the power rectifier can be obtained by summing four components:

$$P_{L,R}(total) = P_{L,R}(on) + P_{L,R}(off) + P_{L,R}(turnon) + P_{L,R}(turnoff) \quad \textbf{[9.13]}$$

The power loss incurred in the power rectifier during the on-state duration from time t_6 to the end of the period is given by:

$$P_{L,R}(on) = \frac{(T - t_6)}{T} . I_M . V_{ON,R} \quad \textbf{[9.14]}$$

In writing this expression, it is assumed that the cycle begins at time t_1. The power loss incurred in the power rectifier during the off-state time duration ($t_4 - t_3$) is given by:

$$P_{L,R}(off) = \frac{(t_4 - t_3)}{T} . I_{L,R} . V_{DC} \quad \textbf{[9.15]}$$

The leakage current ($I_{L,R}$) for the power rectifier will be assumed to be very small allowing this term to be neglected during the power dissipation analysis.

The power loss incurred in the power rectifier during the turn-on event from time t_1 to t_3 can be obtained by analysis of the segments between the time intervals t_1 to t_2 and t_2 to t_3. The power loss incurred during the first segment is much smaller than during the second segment due to the small on-state voltage drop for the power rectifiers. The power loss incurred during the second segment is given by:

$$P_{L,R-2}(turnon) = \frac{1}{2} \frac{(t_3 - t_2)}{T} . I_{PR} . V_{DC} \quad \textbf{[9.16]}$$

The power loss incurred in the power rectifier during the turn-off event from time t_4 to t_6 can be obtained by analysis of the segments between the time intervals t_4 to t_5 and t_5 to t_6. The power loss incurred during the first segment is negligible due to the low leakage current for the power rectifier. The power loss incurred during the second segment is given by:

$$P_{L,R-2}(turnoff) = \frac{1}{2} \frac{(t_6 - t_5)}{T} . I_M . V_{ON,D} \quad \textbf{[9.17]}$$

This power loss is also small due to the low on-state voltage drop of power rectifiers.

In this section, the above power loss analysis is applied to a motor control application using a medium DC-bus voltage with a duty cycle of 50 percent. The DC-bus voltage (V_{DC}) will be assumed to be 400 volts as pertains to the power source in a hybrid electric-car. In this case, the device blocking voltage rating is typically 600 volts. The current being delivered to the motor winding (I_M) will be assumed to be 20 amperes. Due to the larger blocking voltage required for this application, it is commonly implemented using silicon bipolar devices, namely the IGBT as the power switch and the P-i-N rectifier as the fly-back diode.

Characteristics	Silicon IGBT
On-State Voltage Drop (V)	1.8
Turn-Off Time ($t_5 - t_4$) (μs)	0.1
Turn-Off Time ($t_6 - t_5$) (μs)	0.2

Fig. 9.7 Characteristics of IGBTs with 600-V Blocking Voltage Rating.

In the textbook[1], it was demonstrated that the most suitable device for this motor control application is the silicon IGBT. The characteristics of the IGBT that are pertinent to the analysis of the power loss are provided in Fig. 9.7 when the device is operated at an on-state current density of 100 A/cm^2.

Characteristics	Silicon P-i-N	Silicon MPS	4H-SiC JBS
On-State Voltage Drop (V)	0.85	0.87	1.0
Turn-On Time ($t_2 - t_1$) (μs)	0.35	0.25	0.01
Turn-On Time ($t_3 - t_2$) (μs)	0.35	0.25	0.01
Peak Reverse Recovery Current (A)	28	17	2.0

Fig. 9.8 Characteristics of Rectifiers with 600-V Blocking Voltage Rating.

It was also demonstrated in the textbook[1] that the performance of motor control systems can be greatly improved by replacing the silicon P-i-N rectifier with a silicon carbide Schottky rectifier. However, the leakage current for the silicon carbide Schottky rectifier increases by 6 orders of magnitude with increasing reverse bias voltage. This problem can be overcome by using the JBS rectifier concept as shown in chapter 3 of this book. The silicon carbide JBS rectifier is therefore an excellent candidate for motor control applications. However, the cost of silicon carbide rectifiers is at present much greater than that for silicon devices. Consequently, a more attractive approach to reducing power losses in the motor

control applications is by replacing the silicon P-i-N rectifier with a silicon MPS rectifier that was discussed in chapter 7.

The characteristics for the power rectifiers that are pertinent to the analysis of the power loss are provided in Fig. 9.8. All the devices are assumed to be operated at an on-state current density of 100 A/cm^2. The on-state voltage drop, reverse recovery time, and peak reverse recovery current for the silicon P-i-N rectifier and the MPS rectifier are taken from the data provided earlier in chapter 7 (see Fig. 7.35 and Fig. 7.36) for the case of a lifetime of 10 microseconds in the drift region. In the case of the 4H-SiC JBS rectifier structure, the on-state voltage drop is limited by the barrier height for the metal-semiconductor contact due to the low specific on-resistance for the drift region (see Fig. 3.10 for the case of a cell pitch of more than 1.2 microns). The reverse recovery current for the JBS rectifier is assumed to be 10 percent of the on-state current because of the displacement current[4,5].

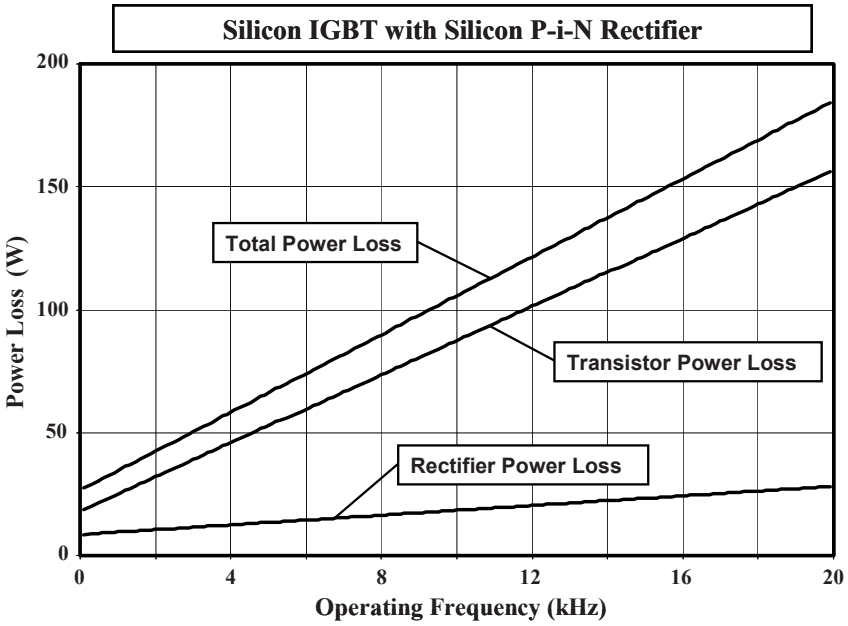

Fig. 9.9 Power Losses during Motor Control with 400-V DC-Bus: Silicon IGBT with Silicon P-i-N Rectifier.

The power losses in the case of the silicon IGBT as the power switch with a silicon P-i-N rectifier as the diode is provided in Fig. 9.9 for frequencies ranging to 20 kHz. The power losses in the transistor are dominant in this case. The power loss in the transistor is larger than in the rectifier at low operating frequencies due to its larger on-state voltage drop. The power loss in the transistor increases rapidly with increasing frequency and becomes the dominant power loss mechanism in

this case. The total power loss for this combination of a silicon IGBT as the switch and the silicon P-i-N rectifier as the diode is 185 watts at 20 kHz when 8000 watts of power is delivered to the load.

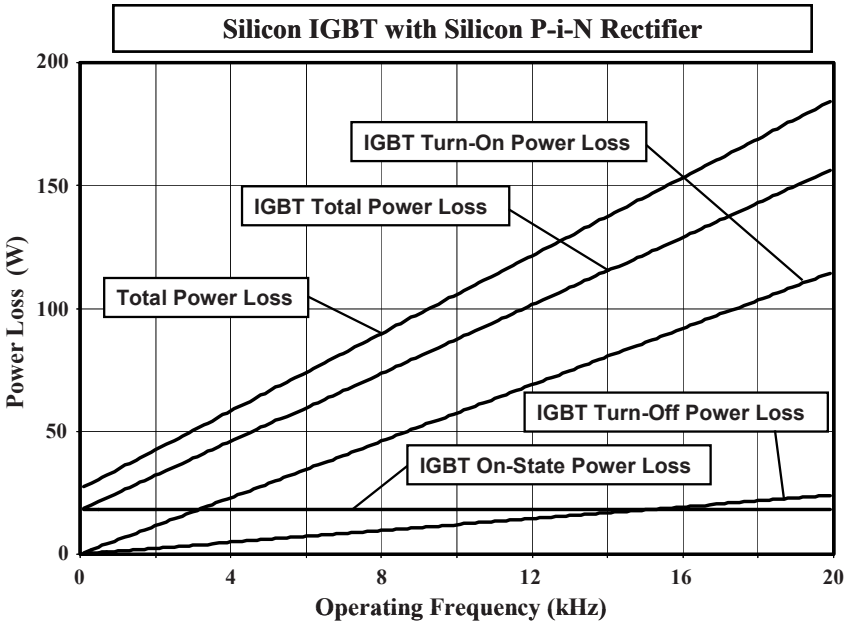

Fig. 9.10 IGBT Power Losses during Motor Control with 400-V DC-Bus: Silicon IGBT with Silicon P-i-N Rectifier.

The components of the power loss within the silicon IGBT are provided in Fig. 9.10 as a function of the operating frequency. From this graph, it is clear that the on-state power loss is dominant up to about 3 kHz. At higher frequencies, the turn-on power loss becomes dominant because it increases rapidly with frequency. This graph demonstrates that the turn-on losses in the IGBT are dominant at high frequencies for this combination of a silicon IGBT as the switch and the silicon P-i-N rectifier as the diode. The high turn-on power losses in the IGBT are produced by the large peak reverse recovery current of the P-i-N rectifier. The large peak reverse recovery current also produces a high current density in the IGBT structure making it prone to latch-up induced failure during operation in the motor control circuit. Based up on these observations, it is clear that improvements in the performance of the power rectifier are required to reduce power losses in the motor control application.

The power losses in the motor control circuit can be reduced by replacing the silicon P-i-N rectifier with a silicon MPS rectifier. The power losses in the case of the silicon IGBT as the power switch with a silicon MPS rectifier as the diode is provided in Fig. 9.11 for frequencies ranging to 20 kHz. The power losses in the

transistor are still dominant in this case. The power loss in the transistor is larger than in the rectifier at low operating frequencies due to its larger on-state voltage drop. The power loss in the transistor increases rapidly with increasing frequency and becomes the dominant power loss mechanism in this case. The total power loss for this combination of a silicon IGBT as the switch and the silicon MPS rectifier as the diode is however reduced to 125 watts at 20 kHz when 8000 watts of power is delivered to the load.

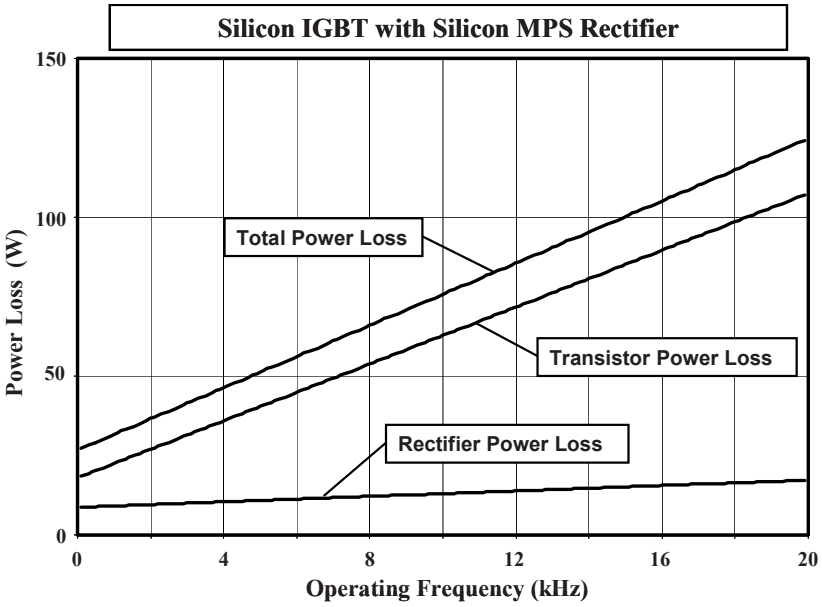

Fig. 9.11 Power Losses during Motor Control with 400-V DC-Bus: Silicon IGBT with Silicon MPS Rectifier.

The components of the power loss within the IGBT are provided in Fig. 9.12 as a function of the operating frequency for the above combination of a silicon IGBT as the switch and the silicon MPS rectifier as the diode. From this graph, it is clear that the on-state power loss is dominant up to about 5 kHz. At higher frequencies, the turn-on power loss becomes dominant because it increases rapidly with frequency. This graph demonstrates that the turn-on losses in the IGBT are still dominant at high frequencies even for this combination of an IGBT as the switch and the MPS rectifier as the diode. The high turn-on power losses in the IGBT are produced by the peak reverse recovery current of the MPS rectifier even though it is smaller than that for the P-i-N rectifier. The reduced peak reverse recovery current of the MPS rectifier makes the IGBT less prone to latch-up induced failure during operation in the motor control circuit. Based up on these observations, it is clear that further improvements in the performance of the power rectifier are required to reduce power losses in the motor control application.

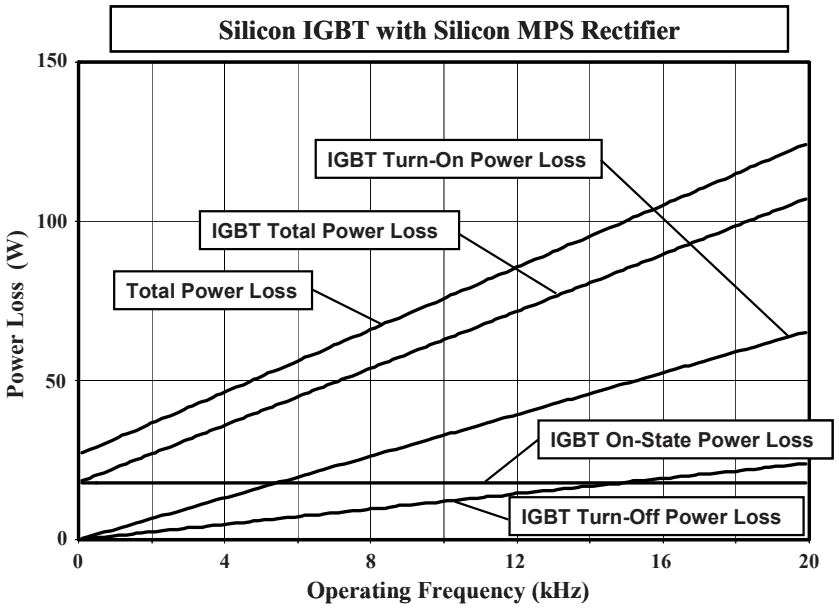

Fig. 9.12 IGBT Power Losses during Motor Control with 400-V DC-Bus: Silicon IGBT with Silicon MPS Rectifier.

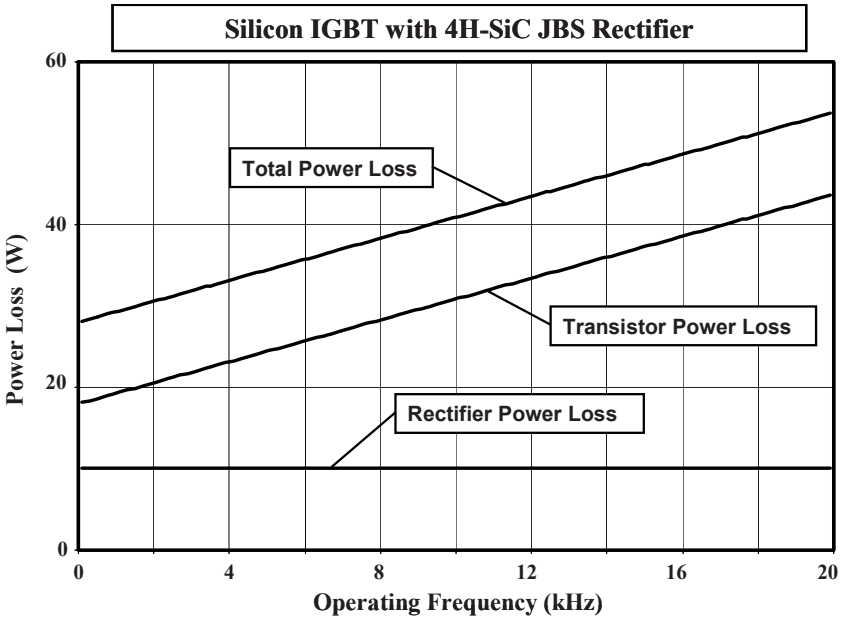

Fig. 9.13 Power Losses during Motor Control with 400-V DC-Bus: Silicon IGBT with Silicon Carbide JBS Rectifier.

An even greater improvement in performance of the motor control system was proposed by replacing the silicon P-i-N rectifier with a silicon carbide Schottky rectifier[3]. Due to the high leakage of the silicon carbide Schottky rectifier, it is only appropriate to consider the silicon carbide JBS rectifier for the motor control applications. The power losses in the case of the silicon IGBT as the power switch with a silicon carbide JBS rectifier as the diode is provided in Fig. 9.13 for frequencies ranging to 20 kHz. The power losses in the transistor are still dominant in this case. The power loss in the transistor is larger than in the rectifier at low operating frequencies due to its larger on-state voltage drop. It can be observed that the power loss in the transistor increases less rapidly with increasing frequency than for the case of the silicon power rectifiers. The total power loss for this combination of a silicon IGBT as the switch and the silicon carbide JBS rectifier as the diode is therefore reduced to 54 watts at 20 kHz when 8000 watts of power is delivered to the load.

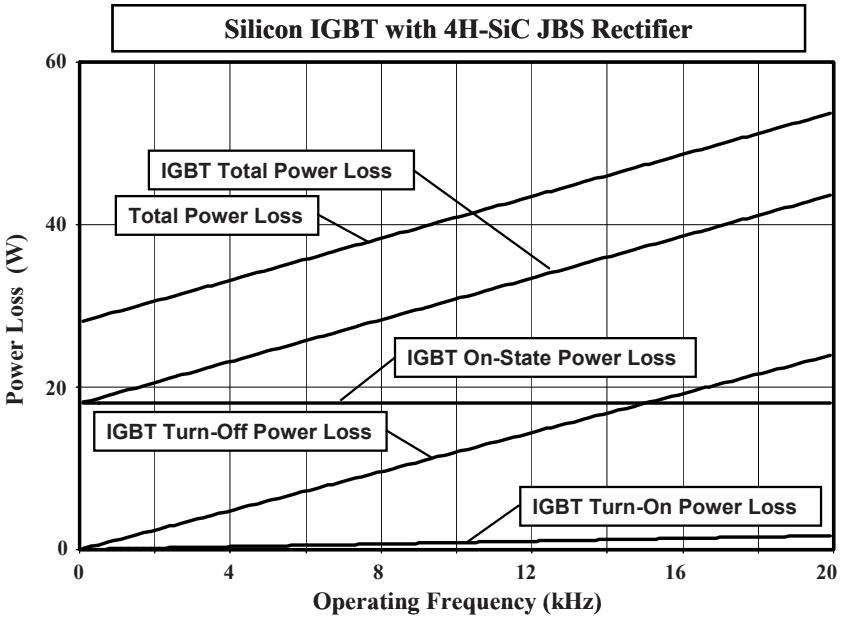

Fig. 9.14 IGBT Power Losses during Motor Control with 400-V DC-Bus: Silicon IGBT with Silicon Carbide JBS Rectifier.

The components of the power loss within the IGBT are provided in Fig. 9.14 as a function of the operating frequency for the above combination of a silicon IGBT as the switch and the silicon carbide JBS rectifier as the diode. From this graph, it is clear that the on-state power loss is dominant up to about 15 kHz. More significantly, the turn-on power loss in the IGBT is now much smaller than the turn-off power loss. This graph demonstrates that the turn-off losses in the IGBT are dominant at high frequencies for this combination of a silicon IGBT as

the switch and the silicon carbide JBS rectifier as the diode. This indicates that further improvements in the performance of the rectifier will not benefit the motor control application. However, replacement of the silicon IGBT with the silicon carbide power MOSFET will produce a significant further reduction of the power losses as shown in the textbook[1].

9.3 Summary

This chapter provides a comparison of the benefits of utilizing various advanced power rectifier concepts that have been described in this book for the typical low voltage DC-to-DC converters for Voltage Regulator Modules (VRMs) and medium voltage motor control applications. It can be concluded that silicon JBS rectifiers can provide a reduction of losses in the VRM application. For the motor control application working from a medium DC-bus voltage, it is advantageous to utilize the silicon MPS rectifier as a low cost technology in the short time frame. In the future, for these applications, silicon carbide JBS rectifiers will greatly reduce power losses when used in conjunction with the silicon IGBT devices as power switches.

References

[1] B.J. Baliga, "Fundamentals of Power Semiconductor Devices", Springer-Science, New York, 2008.
[2] B.K. Bose, "Power Electronics and Variable Frequency Drives", IEEE Press, 1997.
[3] B.J. Baliga, "Power Semiconductor Devices for Variable-Frequency Drives", Proceedings of the IEEE, Vol. 82, pp. 1112-1122, 1994.
[4] P. Brosselard, et al, "Bipolar Conduction Impact on Electrical Characteristics and Reliability of 1.2 and 3.5 kV 4H-SiC JBS Diodes", IEEE Transactions on Electron Devices, Vol. 55, pp. 1847-1856, 2008.
[5] B.A. Hull, et al, "Performance and Stability of Large-Area 4H-SiC 10-kV JBS Rectifiers", IEEE Transactions on Electron Devices, Vol. 55, pp. 1864-1870, 2008.